Photochemical transformation of the insensitive munitions compound 2,4-dinitroanisole

ARTICLE *in* SCIENCE OF THE TOTAL ENVIRONMENT · JANUARY 2013

Impact Factor: 4.1 · DOI: 10.1016/j.scitotenv.2012.11.033 · Source: PubMed

Science of the Total Environment 443 (2013) 692–699

Contents lists available at SciVerse ScienceDirect

Science of the Total Environment

journal homepage: www.elsevier.com/locate/scitotenv

Photochemical transformation of the insensitive munitions compound 2,4-dinitroanisole

Balaji Rao [a,*], Wei Wang [a], Qingsong Cai [b], Todd Anderson [b], Baohua Gu [a,**]

[a] Environmental Sciences Division, Oak Ridge National Laboratory, Oak Ridge, TN, United States
[b] Department of Environmental Toxicology, The Institute of Environment and Human Health, Texas Tech University, Lubbock, TX, United States

HIGHLIGHTS

- DNAN photo-transformation kinetics was dependent on light source and temperature.
- Photolysis produced harmful by-products that included dinitrophenol and nitrate.
- Photo-oxidation was determined to be the likely pathway of DNAN photolysis.

ARTICLE INFO

Article history:
Received 19 March 2012
Received in revised form 3 November 2012
Accepted 6 November 2012
Available online xxxx

Keywords:
Insensitive munitions
2,4-Dinitroanisole
Photo-transformation
Sunlight
Nitrate
2,4-Dinitrophenol

ABSTRACT

The insensitive munitions compound 2,4-dinitroanisole (DNAN) is increasingly being used as a replacement for traditional, sensitive munitions compounds (e.g., trinitrotoluene [TNT]), but the environmental fate and photo-transformation of DNAN in natural water systems are currently unknown. In this study, we investigated the photo-transformation rates of DNAN with both ultraviolet (UV) and sunlight irradiation under different environmentally relevant conditions. Sunlight photo-transformation of DNAN in water was found to follow predominantly pseudo-first-order decay kinetics with an average half-life ($t_{1/2}$) of approximately 0.70 d and activation energy (E_a) of 53 kJ mol^{-1}. Photo-transformation rates of DNAN were dependent on the wavelength of the light source: irradiation with UV-B light (280–315 nm) resulted in a greater quantum yield of transformation ($\phi_{UV\text{-}B} = 3.7\times10^{-4}$) than rates obtained with UV-A light ($\phi_{UV\text{-}A} = 2.9\times10^{-4}$ at 316–400 nm) and sunlight ($\phi_{sun} = 1.1\times10^{-4}$). Photo-oxidation was the dominant mechanism for DNAN photo-transformation, based on the formation of nitrite (NO_2^-) and nitrate (NO_3^-) as major N species and 2,4-dinitrophenol as the minor species. Environmental factors (e.g., temperature, pH, and the presence or absence of naturally dissolved organic matter) displayed modest to little effects on the rate of DNAN photo-transformation. These observations indicate that sunlight-induced photo-transformation of DNAN may represent a significant abiotic degradation pathway in surface water, which may have important implications in evaluating the potential impacts and risks of DNAN in the environment.

Published by Elsevier B.V.

1. Introduction

Defense agencies in the United States and other countries are phasing out the use of certain conventional munitions compounds (e.g., 2,4,6-trinitrotoluene [TNT]) and replacing them with "insensitive" munitions compounds (e.g., 2,4-dinitroanisole [DNAN]) due to safer handling and transporting advantages (Phil and Arthur, 2006; Gray, 2008; Perreault et al., 2012; Xu et al., 2011). An example of an insensitive munitions currently in production is PAX-21 (Picatinny Arsenal eXplosive 21, Picatinny Arsenal, NJ), which is a mixture of DNAN, hexahydro-1,3,5-trinitro-1,3,5-triazine (RDX), n-methyl-p-nitroaniline (MNA) and ammonium perchlorate (Picatinny Arsenal, 2011; Arnett et al., 2009). Historically, DNAN has also been used to manufacture insecticides and azo-dyes (Schechter and Haller, 1944; Fierz-David and Blangey, 1949). As militaries transition from conventional munitions to insensitive munitions, the production, storage and use of DNAN could result in increased occurrences in the environment (e.g., natural water bodies and wastewater systems). Currently, limited information is available on the chronic toxicity of DNAN; although, studies on rats indicated that the acute toxicity of DNAN (LD_{50} = 199 mg/kg) could be even higher than that of TNT (LD_{50} = 794–1320 mg/kg) (Phil et al., 2006). The environmental fate and behavior of DNAN are poorly characterized, and only a few studies have examined the biological transformation of DNAN under aerobic and anaerobic conditions (Perreault et al., 2012; Platten et al., 2010).

Nitroaromatic (e.g., TNT) and nitramine (e.g., RDX) compounds are subject to photo-transformation through sunlight irradiation, affecting the environmental fate, transformation and toxicity of these

* Corresponding author. Tel.: +1 865 574 4727; fax: +1 865 576 8543.
** Corresponding author. Tel.: +1 865 574 7286; fax: +1 865 576 8543.
E-mail addresses: anandharaob@ornl.gov (B. Rao), gub1@ornl.gov (B. Gu).

0048-9697/$ – see front matter. Published by Elsevier B.V.
http://dx.doi.org/10.1016/j.scitotenv.2012.11.033

compounds in surface water bodies (Spanggord et al., 1981, 1983; Mabey et al., 1983). These energetic compounds can undergo photo-transformation through oxidation or reduction of the methyl or nitro groups and polymerization resulting in the formation of nitrobenzenes, nitrophenols, benzaldehydes and azoxydicarboxylic acids (Spanggord et al., 1981, 1983; Mabey et al., 1983). Therefore, understanding the photo-transformation rates, mechanisms and products of DNAN in natural surface water is important to determine its fate in the environment, to evaluate its potential toxicity, and to develop photo-catalyzed remedial technologies (Carp et al., 2004).

In this study, we evaluated the photo-transformation characteristics of DNAN in water, with a particular emphasis on environmental implications. We determined the reaction rates and quantum yields of DNAN photo-transformation with both UV and sunlight sources. Further, the sunlight degradation of DNAN in water was evaluated under different conditions (i.e., temperature, pH, and light intensity). Insights on the reaction mechanisms and products from the photo-transformation of DNAN were obtained with multiple analytical techniques, including reverse-phase high-performance liquid chromatography (RP-HPLC), ion chromatography (IC), UV–visible spectroscopy, Fourier-transform infrared (FTIR) spectroscopy, and liquid chromatography electrospray ion mass spectrometry (LC–ESI-MS).

2. Materials and methods

Reagent grade DNAN ($C_7H_6N_2O_5$, 98% purity, Sigma Aldrich) was used for the preparation of aqueous DNAN stock solutions in distilled deionized water (purity > 18 Ω cm^{-1}, Milli-Q_{PLUS}, Siemens, MA). All chemicals used for the pH adjustments (0.1 N NaOH) and for preparation of the phosphate buffer (0.01 M Na_2HPO_4 and 2×10^{-3} M KH_2PO_4) were of reagent grade or better.

2.1. Photolysis in the ultraviolet (UV) reactor

Photolysis of DNAN in the ultraviolet light region (250–400 nm) was performed separately with two sets of lamps (Luzchem Research, Canada) operating at predominantly UV-A (316–400 nm) and UV-B (280–315 nm) wavelength regimes with peak intensities ~350 and 312 nm, respectively (Fig. 1 and Table 1). A total of 8 lamps (either UV-A or UV-B) were arranged in the overhead slots of a closed UV reactor (Model ICH2, Luzchem Research) about 18 cm from the bottom of the reactor. The inside surface of the reactor was made of unpolished aluminum to enhance diffuse scattering of light. Sample containers were placed upright at the bottom center region of the reactor. A modified ferrioxalate actinometer method (Goldstein and Rabani, 2008) was used to determine the photon flux into the quartz reactor during UV-B and UV-A irradiations. Briefly, 1.5 mL of 0.02 M ammonium ferric sulfate dodecahydrate and 1.5 mL of 0.06 M potassium oxalate monohydrate both in 0.1 N H_2SO_4 were mixed in the dark to form the actinometry solution. After illumination of samples for a predetermined time period, the product Fe^{2+} was analyzed by adding 65 μL of Ferrozine (50 g/L in 0.05 M HEPES buffer) to 3 mL of the actinometry solution (Zepp et al., 1998). The absorbance of the Ferrozine–ferrous complex was measured at a wavelength of 565 nm after a 2-min incubation in the dark. Using the production rate of Fe^{2+} and the surface area to volume ratio of the reaction solution, the photon flux was calculated as 1.4×10^{-5} and 1.1×10^{-5} milli-Einstein cm^{-2} s^{-1} for UV-B and UV-A irradiations, respectively. The temperature inside the reactor was maintained at the set point (ranging from 25 to 35 °C) using a control system connected to a set of internal heating and cooling fans. Quartz cuvettes (3.5 mL) with Teflon caps were filled with solutions of known DNAN concentrations and used for all the kinetic experiments. Samples after irradiation were sacrificed at different time intervals and stored in amber glass containers at 4 °C prior to analysis. Dark control (DC) experiments were conducted in parallel by covering the sample cuvettes with aluminum foil and placing alongside the irradiated samples.

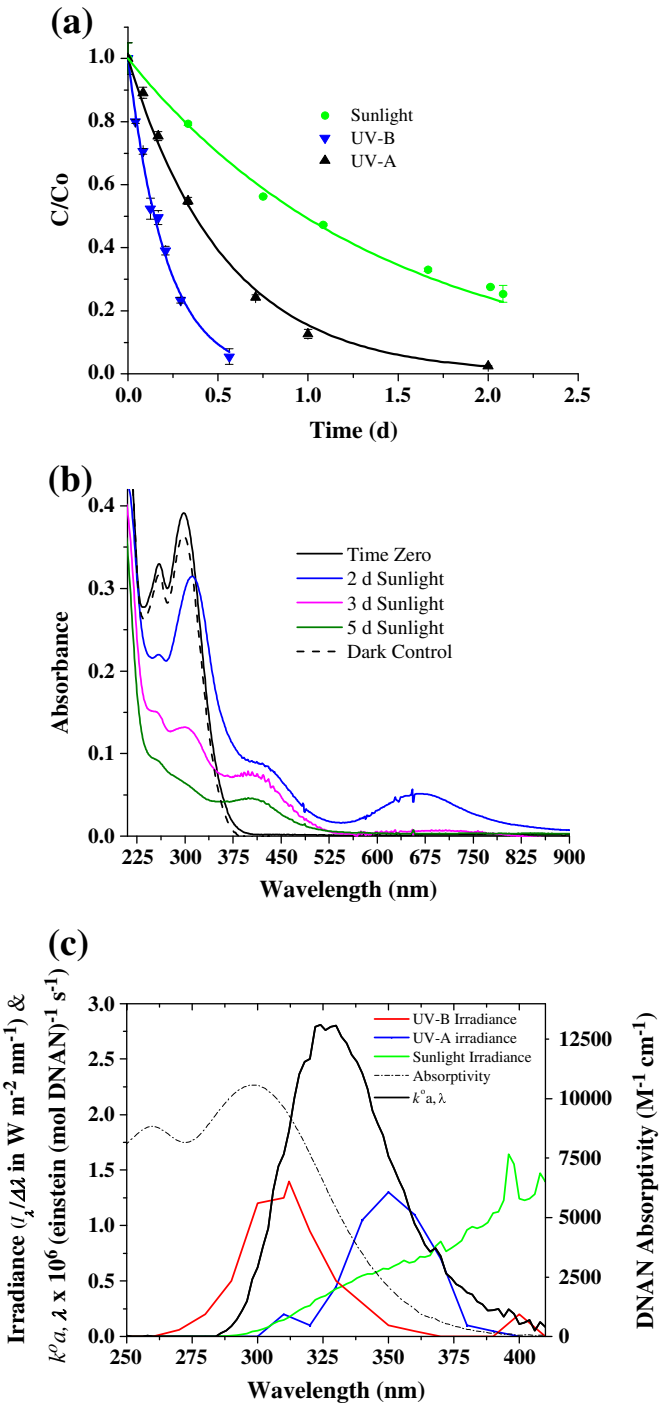

Fig. 1. a) Experimental (symbols) and first-order fitting (lines) results of DNAN photo-transformation under UV-A, UV-B, and solar irradiation normalized to the initial DNAN concentration (C/C_o) (see Table 1 for details). b) UV–visible spectra of DNAN (10 mg L^{-1}) after sunlight photolysis ($\Sigma I_{300-400nm} = 38$ W m^{-2}) at times of 0, 2, 3, and 5 d. c) Spectral irradiance ($I_{\lambda/\Delta\lambda}$) of the lamps used for the photo-transformation experiments and calculated near-surface specific light absorption rate ($k^o_{a,\lambda}$) for the sunlight photolysis of DNAN (right y-axis) and plotted along with molar absorptivity of DNAN (left y-axis).

2.2. Photolysis in a solar simulator

Experiments were also performed under simulated sunlight using a bench-scale solar simulator (SUN TEST XLS+, Atlas-MTS, Germany)

Table 1
Experimental matrix for evaluating the kinetics of DNAN photolysis under different conditions using quartz cuvette.

Evaluated parameter[a]	Initial DNAN concentration (mg L^{-1})	Solvent matrix	Light source	Total UV irradiance (W m^{-2})	Temperature (°C)	pH	First-order rate coefficient (k)[e] d^{-1}	Average half-life ($t_{1/2}$)[e] (d)
Wavelength and light intensity	1.0	DDI[b]	UV-B	49	30 ± 0.2	6.5	6.57 ± 0.15	0.11
	1.0	DDI	UV-A	46	30 ± 0.2	6.5	1.88 ± 0.07	0.37
	1.0	DDI	Sunlight	38	30 ± 1.0	6.5	0.70 ± 0.03	0.99
	1.0	DDI	Sunlight	27	30 ± 1.0	6.5	0.46 ± 0.02	1.51
DNAN concentration	0.1	DDI	Sunlight	38	32 ± 1.0	6.5	1.03 ± 0.07	0.67
	0.5	DDI	Sunlight	38	32 ± 1.0	6.5	1.11 ± 0.05	0.69
	1.0	DDI	Sunlight	38	32 ± 1.0	6.5	0.92 ± 0.05	0.76
	10.0	DDI	Sunlight	38	32 ± 1.0	6.5	0.55 ± 0.05	1.26
pH and ionic strength	1.0	1.0×10^{-3} M PB[c]	Sunlight	38	30 ± 1.0	7.0	0.74 ± 0.03	0.93
	1.0	10^{-6} NaOH[d]	Sunlight	38	30 ± 1.0	8.0	0.84 ± 0.03	0.83
Temperature	1.0	DDI	UV-A	46	25 ± 0.2	6.5	1.37 ± 0.07	0.51
	1.0	DDI	UV-A	46	35 ± 0.2	6.5	2.74 ± 0.10	0.25

[a] All experiments were accompanied with dark controls (no light exposure) that displayed <10% changes in the initial DNAN concentration.
[b] Distilled deionized water containing DNAN at the specified concentration.
[c] Made from stock phosphate buffer solution containing 0.01 M Na_2HPO_4 and 2×10^{-3} M KH_2PO_4.
[d] pH adjusted using a 0.1 N NaOH stock solution.
[e] First-order rate coefficients (k) were obtained by fitting the measured DNAN concentrations using Origin software (OriginPro 8.1 SR2). Half-lives ($t_{1/2}$) in days (d) were calculated using the average modeled first order rate coefficient ($t_{1/2}=0.693/k$).

equipped with a built-in irradiance sensor. The light source was an air-cooled Xenon lamp (1700 W) with a maximum UV (300–400 nm) output of 65 W/m^2 (Fig. 1). A "daylight" filter (Atlas-MTS) was installed in the light source assembly to cut off irradiation at wavelengths <300 nm, thereby simulating typical outdoor sunlight irradiation. Identical to the UV experiments, quartz cuvettes with Teflon caps were used for all the kinetics experiments, and samples were sacrificed at different time intervals and stored in amber glass containers at 4 °C prior to analysis. The exhaust fan system inside the reactor was used to maintain the reactor temperature in a narrow range of ± 1 °C with the average temperature governed by the laboratory conditions (Table 1). All samples and controls were duplicated for each experiment.

2.3. Measurements and characterization of DNAN and its photolysis products

DNAN and its photolysis products were analyzed by a reverse-phase HPLC system connected to a UV–vis variable wavelength detector at 220 nm (Dionex Ultimate 2000™, Dionex Corporation, CA). The separation of DNAN was accomplished using a silica-based analytical column designed especially for analysis of explosives (Acclaim Explosives E2, 5 μm, 4.6×250 mm). Isocratic flow conditions (methanol: water = 1:1) were employed at 1.0 mL min^{-1} and the column was maintained at 30 °C (Chow et al., 2009). All samples including standards were filtered using 0.2-μm Acrodisc syringe filters (13 mm PTFE, PALL Life Sciences) prior to HPLC analysis. The retention time of DNAN was ~16 min using the above conditions (Supplementary data, Fig. S1). Determination of 2,4-dinitrophenol (DNP) formed during DNAN photolysis was accomplished using the methanol–water mixture (1:1) buffered with phosphoric acid as the eluent. The measurement of DNP was verified by monitoring at both 210 nm and 258 nm wavelengths where the molar absorptivity of DNP is the same (Albinet et al., 2010) (see Supplementary data for details). It should be noted that the HPLC columns and analytical conditions used for measurement of DNP and DNAN were different from the one used to identify the photo-transformation intermediates through the ESI-MS and the retention time was different for the compounds analyzed using these systems (see Supplementary text). The quantitative performance of the analytical method was regularly checked with analytical duplicates and standards. The experimental error was generally within ± 12%.

An ion chromatography system equipped with an AS22 anion separation column (ICS-2100, Dionex, Sunnyvale, CA) was used for the measurement of nitrite (NO_2^-) and nitrate (NO_3^-) produced during irradiation of DNAN. Certified NO_2^- and NO_3^- standards (Ricca Chemical, Arlington, TX) were used for the calibration curve from 0.5 to 10 mg L^{-1}. A carbonate/bicarbonate eluent (4.5 mM CO_3^{2-}/1.4 mM HCO_3^-) at a 1.2 mL min^{-1} isocratic flow resulted in the elution of NO_2^- and NO_3^- at 4.7 and 5.8 min, respectively. Identical chromatography conditions were used for analysis of the major anions in the spiked tap water (with 1 mg L^{-1} DNAN). A certified mixed anion standard, including chloride (Cl^-), NO_3^-, and sulfate (SO_4^{2-}), was used for the tap water analysis.

In conjunction with HPLC analysis, spectroscopic techniques, including UV–vis (Hewlett Packard), FTIR (Magna-IR 760 Spectrometer, Nicolet), and LC–ESI-MS, were used to investigate the intermediates and products produced during DNAN irradiation. Sample solutions before and after irradiation at a given time interval were analyzed for UV–vis absorptivity. For FTIR analysis, relatively high DNAN concentrations (30 mg L^{-1}) were used for the irradiation experiment performed in 45-mL quartz flasks. The irradiated samples were sacrificed at different time points and concentrated to dryness using a vacuum freeze dryer. The dried powder was mixed with anhydrous potassium bromide (KBr) and pressed to a pellet before FTIR analysis. One separate sample following sunlight irradiation at 4 d was characterized by LC–ESI-MS to determine reaction products or byproducts (see Supplementary data for details).

3. Results and discussion

3.1. Kinetics of DNAN photolysis under UV-A, UV-B and sunlight irradiation

The kinetics of DNAN photo-transformation predominantly followed first-order transformations, governed by the equation, $C = C_o e^{-kt}$, where C_o and C are the experimentally measured DNAN concentrations at the start of photolysis (t = 0 d) and any given time point (t), respectively. The pseudo first-order rate coefficient (k) was obtained by fitting the measured data points (Figs. 1a and 2). Analysis of all the dark control samples at the end of each experiment exhibited <10% changes in the initial DNAN concentrations, indicating negligible dark (or thermal) transformation. For photolysis reactions, UV-B irradiation was most effective in causing degradation of DNAN at an initial concentration of 1 mg L^{-1}. The first-order rate coefficient (k) was calculated as 6.6 d^{-1} with UV-B light, and this rate was approximately 3.5 and 10 times higher than those values observed under UV-A light (1.9 d^{-1}) and simulated solar irradiation (0.7 d^{-1}), respectively (Fig. 1a and Table 1). The different reaction rates observed with

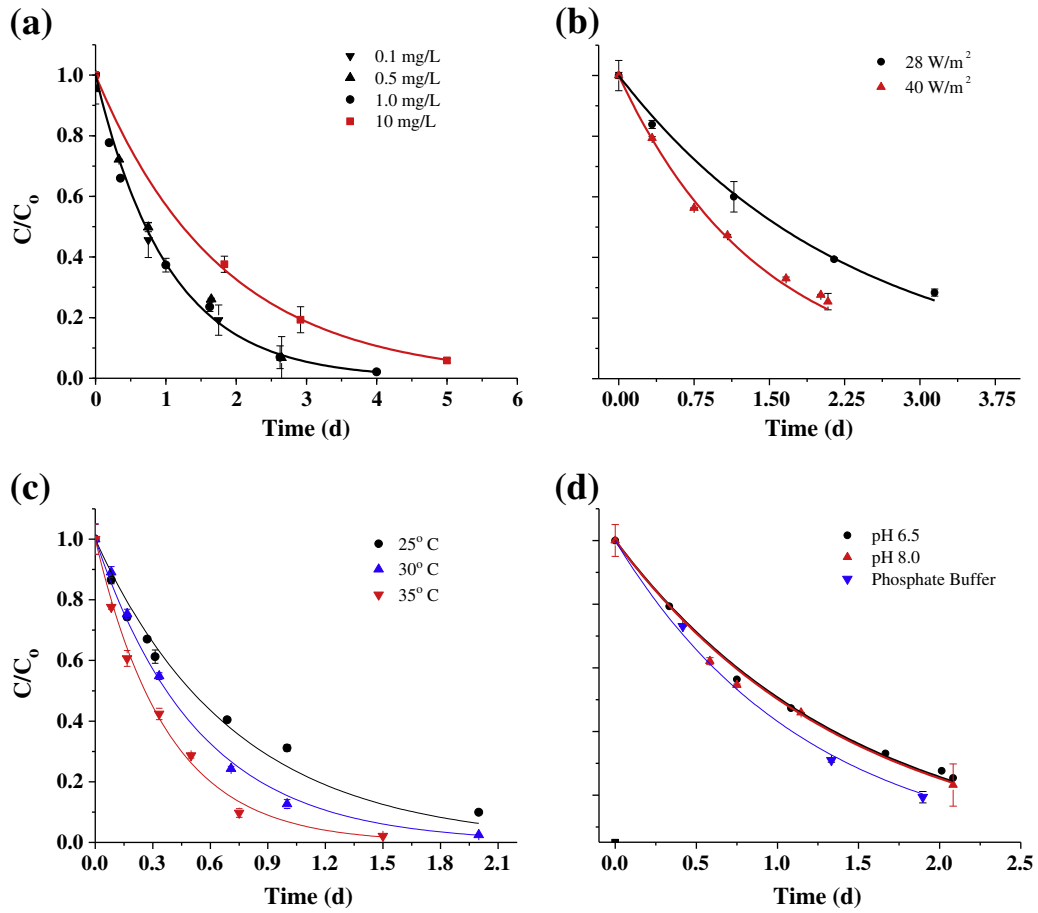

Fig. 2. Experimental (symbols) and first-order fitting (lines) results of DNAN photo-transformation under varying environmental conditions (see Table 1 for details) normalized to the initial DNAN concentration (C/C_o). The error bars are the standard deviation. All experiments were accompanied with dark controls (no light), which displayed <10% change in the initial DNAN concentration.

UV-B, UV-A, and solar light sources could be attributed to variations in lamp intensities as well as the wavelength-specific light absorbance of DNAN. To further understand the effect of the light source (i.e., wavelength) irrespective of the irradiance intensity, the photolysis of DNAN for a given light source was expressed in terms of quantum yield of transformation (ϕ) using the first-order rate coefficient (k) as follows (Eq. (1)),

$$\phi = k/\left(\sum_{\lambda}\left(k^{o}_{a,\lambda}\right)\Delta\lambda\right) \quad (1)$$

where, λ is the wavelength of the incident irradiation (nm), $k^{o}_{a,\lambda}$ is the "near-surface" specific rate (s^{-1} nm^{-1}) of light absorption by DNAN within the wavelength range $\Delta\lambda$, and ϕ is the average quantum yield for the evaluated light source (Schwarzenbach et al., 2003). The $k_{a,\lambda}$ was calculated using the light irradiance (I_λ in photons cm^{-2} s^{-1}) as follows (Eq. (2)),

$$k^{o}_{a,\lambda} = \frac{2.3 \times 1000\ \text{cm}^3\text{l}^{-1}}{6.02 \times 10^{23}\ \text{photons mol}^{-1}}\left(I_\lambda/\Delta\lambda\right)\varepsilon_\lambda \quad (2)$$

where, ε_λ is the decadic molar absorptivity coefficient of DNAN (M^{-1} cm^{-1}) and I_λ is the average spectral irradiance for the range $\Delta\lambda$ (Schwarzenbach et al., 2003). The spectral irradiance at $\Delta\lambda$ values were obtained from the UV and sunlight reactor manufacturers (Fig. 1c). For the photolysis of DNAN under UV-B light, the calculated quantum yield was $(3.7\pm0.2)\times10^{-4}$, which is slightly higher than that obtained under UV-A light ($\phi_{UV\text{-}A}=(2.9\pm0.1)\times10^{-4}$). These calculated values also agree with the low photo-transformation quantum yield ($<10^{-3}$) predicted for 3,5-dinitroanisole, an isomer of DNAN (Cyril et al., 1982). Similarly, using 4-nitroanisole, a compound similar to DNAN with one less nitro group, Simmons and Zepp (1986) reported a quantum yield of 3.2×10^{-4} under direct UV irradiation ($\lambda_{max}=$ 320 nm).

The calculated quantum yield under simulated sunlight irradiation ($\phi_{sun}=(1.1\pm0.1)\times10^{-4}$ nm) was significantly lower than the values for both UV-A and UV-B conditions. It is worth noting that the maximum sunlight $k^{o}_{a,\lambda}$ value shifts to the right of the UV-B, despite a higher absorptivity ($\varepsilon_{\lambda,max}$) of DNAN in that region (Fig. 1c). This effect is due to the greater irradiance of the sunlight spectrum in the UV-A wavelength range than UV-B. The UV fraction of sunlight irradiation at the terrestrial level contains both UV-A (~95%) and UV-B (~5%) but negligible UV-C (Simmons and Zepp, 1986). Furthermore, the UV–visible spectra of DNAN in water displayed major absorbance bands from 200 to 400 nm and negligible absorptions at higher wavelengths (Fig. 1b). The $k^{o}_{a,\lambda}$ was comparatively negligible for sunlight wavelengths greater than 400 nm due to the low DNAN absorptivity at $\lambda>400$ nm. These results indicate that the calculated ϕ_{sun} and $k^{o}_{a,\lambda}$ are useful parameters in evaluating the environmental fate of DNAN under photolytic conditions. They can be used to determine the rate coefficient and predict the half-life of DNAN when exposed to different sunlight intensities and/or water characteristics if the background attenuation coefficient of the natural water source is known (Schwarzenbach et al., 2003).

3.2. Concentration effects and environmental factors for DNAN photolysis

The kinetics of DNAN photo-transformation was subsequently evaluated with varying DNAN concentrations and environmental

conditions (Table 1 and Fig. 2). Under simulated solar light, the average rate constant (k) and half-life ($t_{1/2}$) were found to be 0.98 d^{-1} and 0.7 d, respectively, for initial DNAN concentrations ranging from 0.1 to 1.0 mg/L in water at pH~7 and a temperature of 32±1 °C (Table 1 and Fig. 2a). The fitted rate constant for the highest investigated concentration of DNAN (10 mg/L) resulted in a lower k value (0.55 d^{-1}). The pseudo-first order kinetics for direct photolysis is only applicable when the fraction of light absorbed by DNAN ($F_\lambda = \varepsilon_\lambda C/[\varepsilon_\lambda C + \alpha_\lambda]$, where α_λ is the attenuation coefficient of the background water) is much less than the total light absorbed by the solution ($[\varepsilon_\lambda C + \alpha_\lambda]$) (Schwarzenbach et al., 2003). At 10 mg L^{-1} initial DNAN concentrations, the $\varepsilon_\lambda C$ value (~0.35 for $\lambda = 325$ nm, corresponding to maximum $k^o_{a,\lambda}$ [Fig. 1c]) was sufficiently large (F_λ approaches 1 for $\varepsilon_\lambda C \gg \alpha_\lambda$) to exhibit a mixed order kinetics, involving a zero-order photo-transformation rate at earlier stages of the experiment and switching to a first order rate at DNAN concentrations ≤1 mg L^{-1}. The reduction of the incident sunlight intensity by 30% resulted in a proportionally decreased photo-transformation rate of DNAN by about 35% (Table 1 and Fig. 2b), which is in agreement with the theoretically predicted first order rate coefficient value of 0.49 d^{-1} (calculated with Eq. (2)).

In addition to the light intensity, temperature was found to influence the photo-transformation rate of DNAN under UV-A irradiation (Table 1 and Fig. 2c). The first order rate constants of DNAN photo-transformation increased with higher temperatures: 1.4 d^{-1} at 25 °C, 1.9 d^{-1} at 30 °C, and 3.2 d^{-1} at 35 °C. Using the Arrhenius rate law, the calculated activation energy for the evaluated temperature range was 53±4.0 kJ mol^{-1}. This value is useful to infer the reaction rates at different temperatures (e.g., winter vs. summer seasonal temperatures) that are beyond the temperature range evaluated in our experimental setup. Because the predominant type of UV in sunlight is in the UV-A range, we estimated that the photo-transformation rate of DNAN in winter (~0 °C) would be at least 15 times lower (k~0.17 d^{-1}) than the rate in the hot summer (~35 °C).

Variations in solution pH (from pH 6.5 to 8.0) showed only modest effects on the photo-transformation rate of DNAN in water ($\Delta\ t_{1/2}$ ~ −17%) (Table 1 and Fig. 2d). An increase to pH 8 slightly increased the photo-transformation rate of DNAN (Table 1). The absence of proton exchange sites (e.g., −COOH, $-NH_2$ and −OH) in the DNAN chemical structure may explain why no significant changes in the photolysis rates of DNAN were observed for the evaluated pH range (Fig. 2d). This result indicates that, under typical environmental conditions, pH does not significantly alter the direct photolysis rate of DNAN; although, it does not rule out possible effects of extreme pH (pH<6 and >8) on photolysis. We also evaluated the possible effects of naturally dissolved organic matter (DOM) on the photo-transformation of DNAN in water. Results (Supplementary data Fig. S2) showed essentially no change in DNAN kinetics for either tap water or samples spiked with up to 10 mg L^{-1} Suwannee River DOM, an unfractionated reference organic matter obtained from the International Humic Substances Society (IHSS).

The sunlight photolysis half-life of DNAN is within the range of other energetic compounds, including TNT, RDX and HMX with average

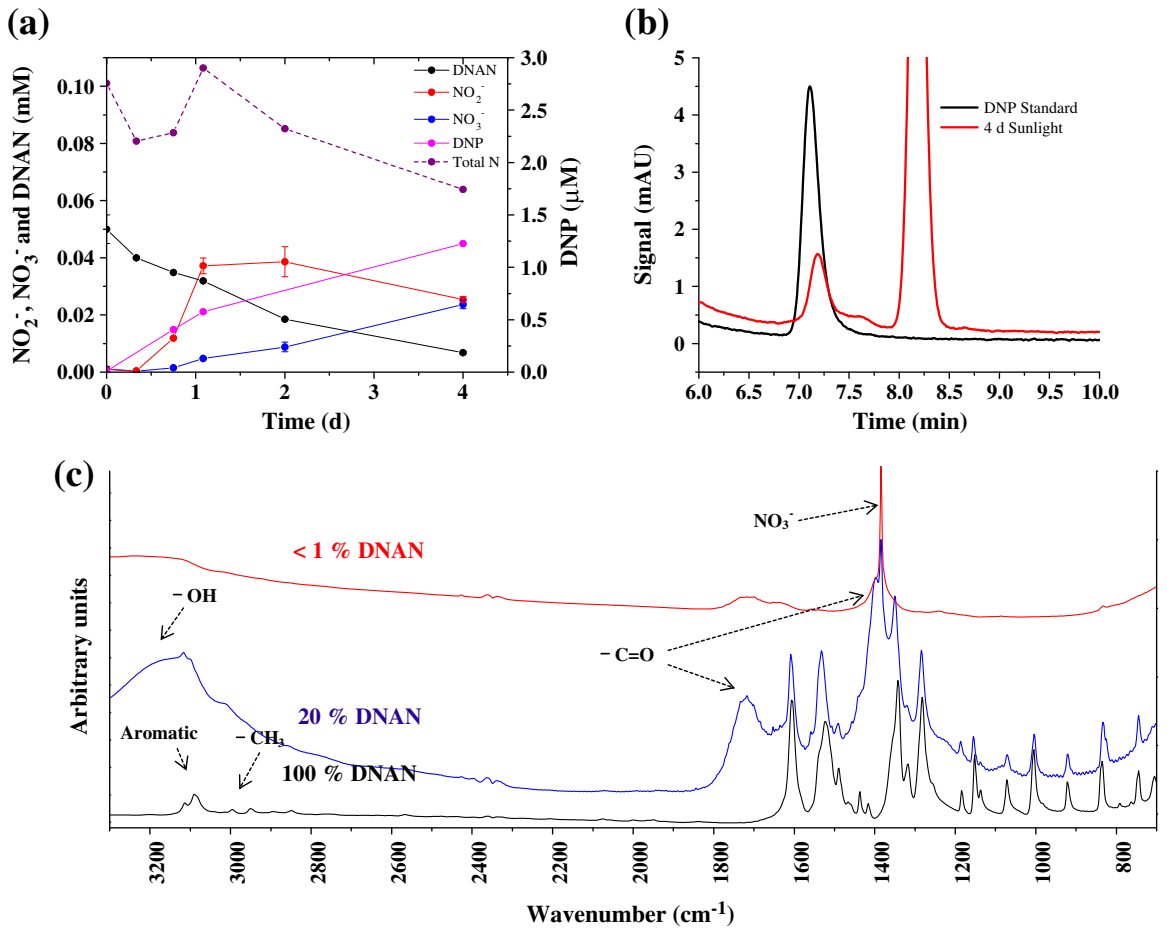

Fig. 3. a) Production of NO_2^-, NO_3^- and DNP (represented as % N of starting DNAN) during sunlight photolysis (~40 W m^{-2}, 300–400 nm) of 10 mg L^{-1} DNAN (100% N at time = 0 d) at 30 °C. b) Chromatograph of 2,4-dinitrophenol (DNP) produced after sunlight photolysis of DNAN (38 W m^{-2} and 4 d) and overlaid on a standard solution of DNP (blue line). c) Fourier transform infrared (FTIR) spectra of DNAN before (black solid line) and after photolysis (5 d, blue line and 12 d, red line) corresponding to 0%, 20% and <1% DNAN remaining in the solution, respectively. (For interpretation of the references to color in this figure legend, the reader is referred to the web version of this article.)

photolysis half-lives ($t_{1/2}$) of 0.5, 0.8, and 2.3 d, respectively (Spanggord et al., 1981, 1983; Mabey et al., 1983). The measured k of DNAN is similar in magnitude to the reported first-order rate constants for TNT of 0.86 and 8.6 d^{-1} under sunlight and UV ($\lambda_{max} = 313$ nm), respectively, at an initial concentration ≤ 1 mg L^{-1} TNT in water (Spanggord et al., 1981, 1983; Mabey et al., 1983).

3.3. Photo-transformation products and pathways of DNAN

Identification of the intermediates and products formed during DNAN photo-transformation is important from a theoretical perspective as well as in regards to toxicological impacts on water quality. The major reaction intermediates and products identified during both sunlight and UV photolysis of DNAN were nitrite (NO_2^-), nitrate (NO_3^-) and minor amounts of 2,4-dinitrophenol (Figs. 3 and S3). The amounts of NO_2^- and NO_3^- produced accounted for most of the N fraction (>60%) in the sunlight irradiation of DNAN (Fig. 3a). These results indicated the cleavage of nitro-groups on the benzene ring structure during DNAN photolysis. The concentration of NO_2^- increased during the earlier periods of DNAN sunlight photo-transformation (<1 d), reached a plateau, and then decreased at later time points (>2 d) (Fig. 3a). These results indicated that NO_2^- is one of the major reaction intermediates. On the other hand, NO_3^- concentration showed a steady increase during the entire photolysis period, suggesting that it is one of the reaction end products because NO_2^- is unstable and can be oxidized to NO_3^-. Similarly, NO_2^- and NO_3^- products accounted for nearly 100% of the N removed from DNAN during both UV-B and UV-A irradiation, demonstrating a negligible presence of other N-containing compounds (Supplementary data Fig. S3).

The production of DNP under sunlight irradiation (Fig. 3a), albeit at low concentrations (<3% of total N), in the irradiated solutions indicated splitting of CH_3O- group in DNAN, which likely resulted in the formation of methanol (CH_3OH) (Fig. 3a). DNP is an important reaction intermediate and can undergo further photolysis to release NO_2^- into the solution (Alif et al., 1991; Ishag and Moseley, 1977). Identification of DNP was obtained from both HPLC-UV and LC–ESI-MS analyses (Figs. 3b and S4). The time-resolved mass scans (deprotonated molecular mass $[M-H]^-$ at m/z = 50 to 450 Da) displayed major abundances at 183 Da, which corresponded to deprotonated DNP after 4 d of sunlight irradiation.

In addition to the identified NO_2^-, NO_3^- and DNP species in the sunlight irradiated solutions, FTIR and LC–MS indicated the presence of several other reaction products or byproducts (Figs. 3c and S4). FTIR analysis of the sunlight irradiated samples taken at 5 d and 12 d (corresponding to 20% and <1% DNAN remaining in solution), revealed a broad peak between 3000 and 3300 cm^{-1}, indicating the presence of –OH groups (Fig. 3c). A sharp absorption peak at ~1385 cm^{-1} for both the samples is characteristic of inorganic NO_3^- salts (Fig. 3c) (Wade, 1999). The appearance of moderate peaks at 1650–1750 cm^{-1} and 1350–1450 cm^{-1} for the 5 d sample demonstrated the existence of –COOH or –C=O containing compounds (Wade, 1999), further indicating photo-chemically-induced oxidation of DNAN. However, these peaks essentially disappeared following a prolonged sunlight exposure (12 d, corresponding to <1% of DNAN remaining in solution), which also caused the decrease or disappearance of peaks corresponding to aromatic (3000–3200 cm^{-1}) and $-CH_2/-CH_3$ groups (2800–3000 cm^{-1}). These results indicated that the cleavage of DNAN produced lower molecular weight compounds

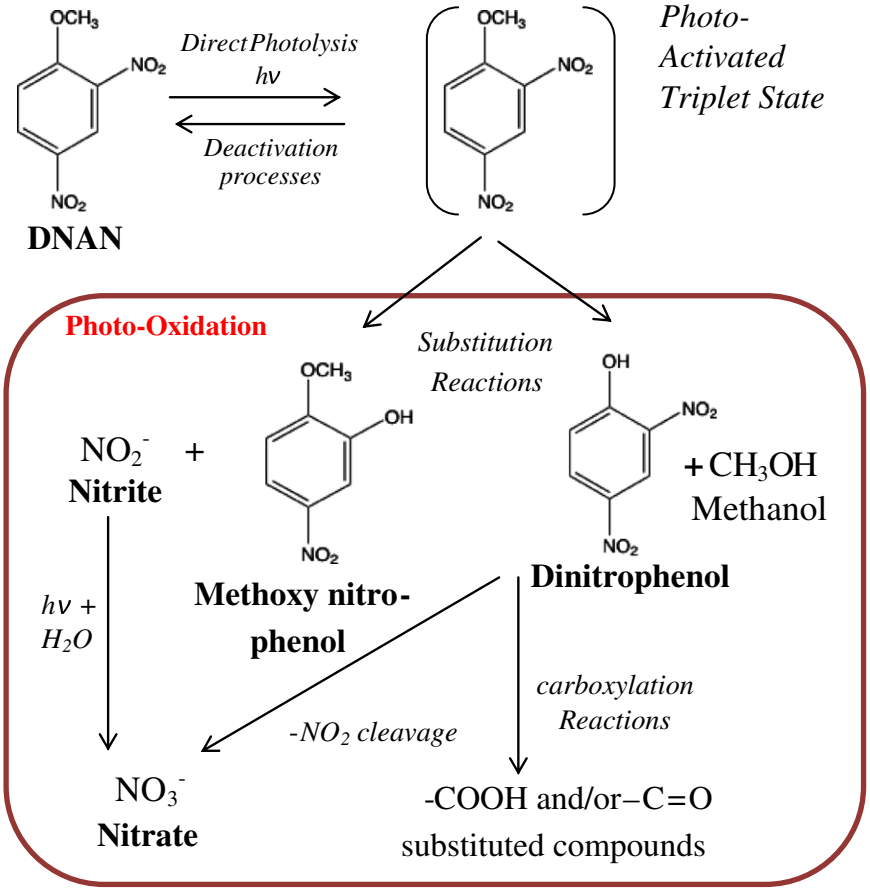

Fig. 4. Sunlight photo-transformation pathways of DNAN based on the results obtained from IC, HPLC, LC–MS and FTIR analyses. Photo-transformation of DNAN resulted mainly in the formation of oxidation products. The formation of –COOH and –C=O substituted compounds is indicated in the FTIR analysis of phototransformed DNAN (see Fig. 3c).

(Fig. 3c). The results of the LC–MS analysis demonstrate the presence of methoxy-nitrophenols ($[M-H]^-$ at 168 Da), dinitrophenol ($[M-H]^-$ at 183 Da), nitroso-anisole ($[M-H]^-$ at 181 Da), amino substituted nitrophenol ($[M-H]^-$ at 153 Da), and their corresponding isomers (Supplementary data Fig. S4). The presence of nitrophenol and its methoxy derivatives are also shown in the FTIR spectroscopic analyses (Fig. 3c). The absence of major peaks that correspond to $-NH_2$ or NH_4^+ groups in the FTIR analyses despite the identification of amino-nitrophenol in the ESI-MS could be because of the relatively lower sensitivity of the FTIR.

Overall, our results indicate that photo-oxidation is largely responsible for aqueous DNAN photo-transformation under oxic conditions, which is underscored by the presence of NO_2^- and NO_3^- as dominant N species and the existence of $-COOH$ or $-C{=}O$ containing compounds in the irradiated products. Fig. 4 illustrates the proposed reaction pathways for the photolysis of DNAN. In a study on the photolysis of 3,5-dinitroanisole in alkaline solutions, Cyril et al. (1982) reported the replacement of both CH_3O- and NO_2 groups with $-OH$ through an S_N2 type substitution process. Similarly, the photolysis of DNAN is expected to result in a photo-excited state (triplet) that undergoes photo-substitution (S_N2 type) by OH^- to form nitrophenol and its methoxy derivatives (Fig. 4) (Cyril et al., 1982; van Reil et al., 1981; Havinga and Cornelisse, 1976; Evans et al., 1997). The increase in the DNAN photo-transformation kinetics at the evaluated pH of 8 (Fig. 2d) supports the involvement of OH^- ion. Methoxy-nitrophenols and nitrophenols can undergo further photo-oxidation to form $-COOH$-containing compounds (e.g., cyclopentadiene carboxylic acids) and NO_2^- or NO_3^- (Fig. 4), which is consistent with the results obtained in the IC and FTIR analyses (Alif et al., 1991). Previous studies have shown that reductive transformation of DNAN is the major process by bacterial degradation under anaerobic conditions (Perreault et al., 2012; Platten et al., 2010), but this pathway would be less likely in oxygenated water under UV and sunlight photolysis conditions, as used in our experiments.

4. Conclusion

Despite the growing interest in the production and use of insensitive munitions, significant knowledge gaps exist on the potential impacts of DNAN contamination in the environment. Our results indicate that sunlight-induced photolysis of DNAN is a rapid process with an average half-life ranging from 0.6 to 1.0 d. The kinetics of the photo-transformation are faster than the reported biotransformation rate of DNAN under anaerobic conditions (Perreault et al., 2012); thus, photo-transformation might be especially important in light-exposed environments, such as shallow surface water or surface soil (Balmer et al., 2000). Although the present study primarily focused on the photolysis of DNAN in water, similar reactions could be anticipated on soil surfaces, possibly with even faster degradation rates due to surface-catalyzed reactions (Schmelling and Gray, 1995). This assumption is supported by the results that DNAN photo-transformation rates were increased by nearly two orders of magnitude in the presence of anatase (TiO_2) colloidal particles (Fig. 5), demonstrating its potential as a remedial technology for DNAN-contaminated soil and water. However, evaluation of the photocatalytic transformation of DNAN in a heterogeneous medium would require detailed characterization of the photoactive particles and their interactions with the solution, which is beyond the scope of this paper.

Our results also indicate that sunlight-induced photolysis of DNAN might represent a major abiotic transformation pathway and should be considered in evaluating its potential impacts and risks at contaminated sites. The quantum yield of DNAN photo-transformation in conjunction with the calculated activation energy obtained in this study can be useful in predicting the fate of DNAN in surface water. The identified products and intermediates (e.g., NO_3^-, DNP, and NO_2^-) are known to impart significant ecotoxicities. In particular, DNP is a highly toxic compound that is a powerful phosphorylation uncoupling agent and has an EPA reference dose for chronic oral exposure of ≤ 2 μg kg^{-1} d^{-1} (Hassio et al., 2002; US EPA, 2011). This dose corresponds to a drinking water concentration of ~70 μg L^{-1}, which was readily produced during exposure of a 10 mg L^{-1} DNAN solution to sunlight in this study.

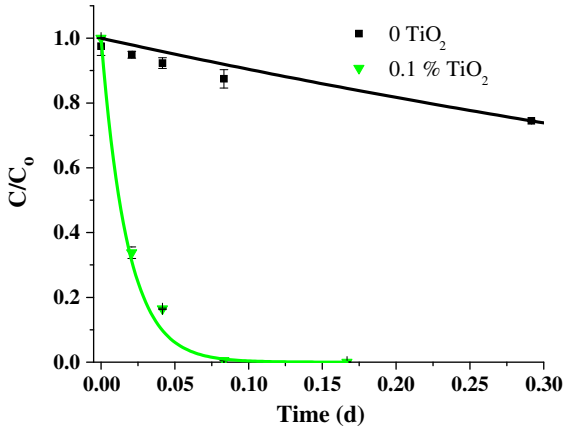

Fig. 5. Comparison of the UV-B photolysis of DNAN in the absence and presence (0.1% and 1%) of TiO_2-anatase suspensions.

Acknowledgments

We thank Donna Kridelbaugh of ORNL for her technical editing of the manuscript. We also thank Xiangping Yin and Prasesh Sharma of ORNL for their help with the HPLC analysis. This research was supported in part by the Strategic Environmental Research and Development Program (SERDP) of the U.S. Department of Defense. Oak Ridge National Laboratory is managed by UT-Battelle, LLC for the U.S. Department of Energy under contract DE-AC05-00OR22725.

Appendix A. Supplementary data

Supplementary data to this article can be found online at http://dx.doi.org/10.1016/j.scitotenv.2012.11.033.

References

Albinet A, Minero C, Vione D. Photo-transformation processes of 2,4-dinitrophenol, relevant to atmospheric water droplets. Chemosphere 2010;80:753–8.
Alif A, Pilichowski J-F, Boule P. Photochemistry and environment XIII: photo transformation of 2-nitrophenol in aqueous solution. J Photochem Photobiol A Chem 1991;59:209–19.
Arnett C, Rodriguez G, Maloney SW. Analysis of bacterial community diversity in anaerobic fluidized bed bioreactors treating 2,4-dinitroanisole (DNAN) and *n*-methyl-4-nitroaniline (MNA) using 16S rRNA gene clone libraries. Microbes Environ 2009;24:72–5.
Balmer ME, Goss K-U, Schwarzenbach RP. Photolytic transformation of organic pollutants on soil surfaces — an experimental approach. Environ Sci Technol 2000;34:1240–5.
Carp O, Huisman CL, Reller A. Photoinduced reactivity of titanium dioxide. Prog Solid State Chem 2004;32:33-177.
Chow TM, Wilcoxon MR, Piwoni MD, Maloney SW. Analysis of new generation explosives in the presence of U.S. EPA Method 8330 energetic compounds by high-performance liquid chromatography. J Chromatogr Sci 2009;47:41–3.
Cyril AG, Varma O, Tamminga JJ, Cornelisee J. Mechanistic and kinetic aspects of the photoinduced OCH_3 substitution in 3,5-dinitroanisole. J Chem Soc Faraday Trans 1982;78:265–84.
Evans CH, Árnadóttir G, Scaiano JC. Reactivity of the 3-nitroanisole triplet: methanol inhibition of photohydroxylation. J Org Chem 1997;62:8777–83.
Fierz-David HE, Blangey L. Fundamental processes of dye chemistry. New York, U.S.A.: Interscience Publishers, Inc.; 1949
Goldstein S, Rabani J. The ferrioxalate and iodide-iodate actinometry. J Photochem Photobiol A Chem 2008;193:50–5.
Gray N. Insensitive munitions — new explosives on the horizon. Fort Belvoir, VA: Army Acquisition, Logistics & Technology (AT&L); 2008. http://asc.army.mil/docs/pubs/alt/2008/1_JanFebMar/articles/34_Insensitive_Munitions-_New_Explosives_on_the_Horizon_200801.pdf.

Hassio K, Nissinen E, Sopanen L, Heinonen EH. Different toxicological profile of two COMT inhibitors in vivo: the role of uncoupling effects. J Neural Transm 2002;109: 1391–401.
Havinga E, Cornelisse J. Aromatic photosubstitution reactions. Pure Appl Chem 1976;47: 1-10.
Ishag MIO, Moseley PGN. Effects of UV light on dilute aqueous solutions of m- and p-nitrophenol. Tetrahedron 1977;33:3141–4.
Mabey WR, Tse D, Baraze A, Mill T. Photolysis of nitroaromatics in aquatic systems. Chemosphere 1983;12:13–6.
Perreault NN, Manno D, Halasz A, Thiboutot S, Ampleman G, Hawari J. Aerobic biotransformation of 2,4-dintiroanisole in soil and soil *Bacillus* sp. Biodegradation 2012. http://dx.doi.org/10.1007/s10532-011-9508-7.
Phil JD, Arthur P, Australian Government Department of Defense. Characterisation of 2,4-dinitroanisole: an ingredient for use in low sensitivity melt cast formulations. Edinburgh, South Australia: Defense Science and Technology Organisation; 2006 [www.dspace.dsto.defence.gov.au/dspace/bitstream/1947/4431/1/DSTO-TR-1904.PR.pdf].
Picatinny Arsenal. Products and services. http://www.pica.army.mil/PicatinnyPublic/products_services/products06.asp 2011.
Platten WE, Bailey D, Suidan MT, Maloney SW. Biological transformation pathways of 2,4-dinitro anisole and N-methyl paranitro aniline in anaerobic fluidized-bed bioreactors. Chemosphere 2010;81:1131–6.
Schechter MS, Haller HL. Colorimetric determination of 1-chloro-2,4-dinitrobenzene as an impurity in 2,4-dinitroanisole. Ind Eng Chem 1944;16:326–7.
Schmelling DC, Gray KA. Photocatalytic transformation and mineralization of 2,4,6-trinitrotoluene (TNT) in TiO_2 slurries. Water Res 1995;29:2651–62.
Schwarzenbach RP, Gschwend PM, Imboden DM. Environmental organic chemistry. 2nd ed. New York: Wiley-Interscience Publishers; 2003.
Simmons MS, Zepp RG. Influence of humic substances on photolysis of nitroaromatic compounds in aqueous systems. Water Res 1986;20:899–904.
Spanggord RJ, Mabey WR, Mill T, Chou T, Smith JH, Lee S. Environmental fate studies on certain munitions wastewater constituents. Phase III, part II — laboratory studies. Report no. LSU 7934. Frederick, Maryland: U. S. Army Medical Research and Development Command; 1981.
Spanggord RJ, Mabey WR, Chou T, Lee S, Alferness PL, Tse DS, et al. Environmental fate studies of HMX. Phase II — detailed studies. Report no. LSU 4412. Frederick, Maryland: U. S. Army Medical Research and Development Command; 1983.
U.S. Environmental Protection Agency. Integrated risk information system: 2,4-dinitrophenol. http://www.epa.gov/iris/subst/0152.htm#oralrfd 2011.
van Reil HCHA, Lodder RG, Havinga E. Photochemical methoxide exchange in some nitromethoxybenzenes. The role of the nitro group in S_N2Ar^* reactions. J Am Chem Soc 1981;103:7257–62.
Wade LG. Organic chemistry. New Jersey: Prentice-Hall, Inc.; 1999.
Xu Z, Hao J, Braida W, Strickland D, Li F, Meng X. Surface-enhanced Raman scattering spectroscopy of explosive 2,4-dinitroanisole using modified silver nanoparticles. Langmuir 2011;27:13773–9.
Zepp RG, Gumz MM, Miller WL, Gao H. Photoreaction of valerophenone in aqueous solution. J Phys Chem A 1998;102:5716–23.